Structural and electronic properties of the ordered double perovskites A_2MReO_6 (A=Sr,Ca; M=Mg,Sc,Cr,Mn,Fe,Co,Ni,Zn)

H. Kato,* T. Okuda,† Y. Okimoto, and Y. Tomioka
Correlated Electron Research Center (CERC), National Institute of Advanced Industrial Science and Technology (AIST), Tsukuba 305-8562, Japan

K. Oikawa‡ and T. Kamiyama
Institute of Materials Structure Science, KEK, Tsukuba 305-0801, Japan

Y. Tokura
Correlated Electron Research Center (CERC), National Institute of Advanced Industrial Science and Technology (AIST), Tsukuba 305-8562, Japan;
Spin Superstructure Project, ERATO, Japan Science and Technology Corporation (JST), Tsukuba 305-8562, Japan;
and Department of Applied Physics, University of Tokyo, Tokyo 113-8656, Japan

(Received 2 December 2003; published 19 May 2004)

Structural and electronic properties have been investigated for a series of Re-based ordered double perovskites, A_2MReO_6 (A=Sr,Ca; M=Mg,Sc,Cr,Mn,Fe,Co,Ni,Zn), which contain some prospective candidates of the high-temperature half-metals for future spin-electronic use. Neutron diffraction measurements have revealed the variation of the Re-O bond length with the change of its effective valence states depending on the counter M ion, namely, Re^{6+}- or Re^{5+}-based insulating states, or otherwise mixed-valent metallic (or barely Mott-insulating) states. Magnetotransport and specific heat studies have clarified metal-insulator phenomena for M=Cr and Fe compounds with the change of A site as well as the intergrain tunneling magnetoresistance characteristic of the ceramics of half-metal oxides.

DOI: 10.1103/PhysRevB.69.184412 PACS number(s): 75.47.−m, 71.30.+h, 61.12.Ld

I. INTRODUCTION

In ordered double perovskite (ODP) structure denoted as $A_2B'B''O_6$ (A being an alkaline-earth or rare-earth ion), the transition-metal sites (perovskite B sites) are occupied alternately by different cations B' and B'' as schematically shown in Fig. 1. Among them, Sr_2FeMoO_6 (Ref. 1) and Sr_2FeReO_6 (Refs. 2,3) have been known as prospective magnetoelectronic compounds, which show tunneling type magnetoresistance at room temperature in polycrystalline form. These features have been ascribed to their highly spin-polarized (or half-metallic) nature and high-magnetic Curie temperature. In those metallic compounds, Fe^{3+} ($3d^5$, $S=5/2$) spins are tied ferromagnetically via the coupling with the conduction electron mainly on Mo^{5+} (or Re^{5+}) sites. Thus, the conduction band is mainly composed of the $4d$ (or $5d$) down-spin electrons of Mo^{5+} (or Re^{5+}).

In the case of Sr_2MMoO_6, when a transition metal (M) prefers a divalent state such as Mn, Co, and Ni, Mo ion becomes nominally hexavalent or nonmagnetic and M ions couple with each other in a weakly antiferromagnetic manner. This results in the G-type antiferromagnetic ground state with a relatively low Neel temperature ($\leqslant$34 K) except Sr_2NiMoO_6 (T_N=80 K).[4,5] In the case of A_2MReO_6, by contrast, a divalent magnetic M ion and Re^{6+} ($5d^1$, $S=1/2$) couple antiferromagnetically, and the compounds show ferrimagnetic properties. Thus, it is anticipated that Re-based ODP's may show even a more variety of magnetic properties than the Mo-based ones. Sleight and co-workers did the first systematic study on Re-based ODP's in 1960s.[6,7] They synthesized a variety of Re-based compounds in polycrystalline form as well as single-crystals of Ba_2MReO_6 (M=Mn,Fe,Co,Ni,Mg,Y) hydrothermally, and reported their structural and magnetic properties. They have also reported a ferromagnetic metallic nature for M=Fe and ferromagnetic insulating nature for M=Mn and Ni. As for the magnetic properties of other Re-based ODPs, Khattak *et al.* revealed a spin helical structure in Ba_2CoReO_6 by a powder neutron diffraction study.[8] Sr_2CaReO_6 has been reported as the $S=1/2$ geometrical spin frustration system, where a localized Re^{6+} t_{2g}^1 electron or $S=1/2$ spin forms fcc lattice in the ODP structure.[9] Concerning the transport characteristics, we have recently reported the bandwidth-control metal-insulator transition for $(Sr,Ca)_2MReO_6$ (M=Cr,Fe).[10,11] In particular, we have found that Sr_2CrReO_6 has the highest Curie temperature (T_C) of 635 K among the perovskite-type oxide materials.[11]

From the viewpoint of the prospective magnetoelectronic materials, we have here systematically investigated the detailed lattice structures and electronic properties of Re-based ODP's, A_2MReO_6 (A=Ca,Sr; M=Mg,Sc,Cr,Mn,Fe,Co,Ni,Zn). We have found almost all the compounds show insulating properties except Sr_2FeReO_6, Sr_2CrReO_6, and Ca_2FeReO_6. The metal-insulator phenomena in these Re-based ODP's are discussed in terms of the valence-dependent electronic configuration of the transition-metal components.

II. EXPERIMENT

Polycrystalline samples of Sr_2MReO_6 (M=Mg,Sc, Cr,Mn,Fe,Co,Ni,Zn) and Ca_2MReO_6 (M=Cr,Mn,Fe,Co,

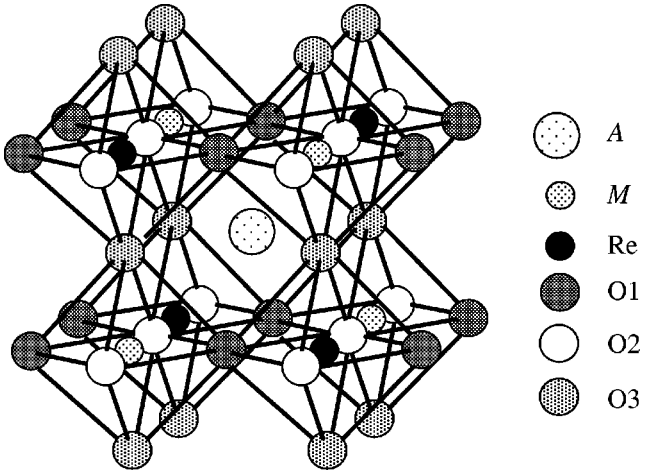

FIG. 1. Schematic structure of the ordered double perovskite A_2MReO_6.

Ni) were synthesized by solid-state reaction. The mixture of SrO, CaO, MO_x, Re_2O_7, and Re were weighted to a prescribed molar ratio and fired at 1173 K in evacuated silica tubes. Then, the samples were regrounded, pelletized, and sintered at 1373–1673 K in Ar atmosphere or evacuated silica tubes. Obtained samples were almost single phase with a trace of impurities (less than 2% in fraction) except Ca_2NiReO_6 (about 8%).

Crystal structures were at first checked by powder x-ray diffraction. The powder neutron diffraction measurements were also carried out at room temperature to determine precise lattice structures including oxygen positions using diffractometers, Sirius[12] and Vega[13] at the pulsed spallation neutron facility, KENS, in High energy Accelerator Research Organization, Japan. Structural parameters, including the *B*-site (*M* and Re) ordering, were refined by the Rietveld method with the program of RIETAN-2001T.[14] The resistivity was measured on the sintered sample with a standard four-probe technique. The magnetization was measured with a commercial superconducting quantum interference device magnetometer. The low-temperature specific heat below 20 K was measured by a relaxation method to evaluate the electronic specific heat coefficient γ.

III. RESULTS AND DISCUSSION

A. Crystal structures

Structural properties as determined by powder neutron diffraction measurements at room temperature for various ODP's are summarized in Table I. We could not deduce the accurate lattice parameters for Ca_2NiReO_6 because of the inferior quality of the specimen. All the perovskite compounds are almost fully *B*-site ordered except Sr_2CrReO_6 and Ca_2CrReO_6 (with the site ordering of 76.6% and 85.3%, respectively). Sr_2ZnReO_6 compound has two phases at room temperature, one is tetragonal and the other is monoclinic phase.

To investigate the valence states of *B*-site ions in ODP's, the bond-valence sums (*V*) were calculated from the Re-O and *M*-O bond lengths. The bond-valence S_{ij} between the ith and jth atoms is defined as $S_{ij}=\exp\{(d_0-d_{ij})/0.37\}$.[15] Here, d_{ij} is the bond length between the ith and jth atoms and d_0 is the bond-valence parameter that has been empirically determined for the i-j pair.[15] They both are in units of Å. The effective valence of the ith metal element is given by the bond-valence sum, $V_i=\Sigma_j S_{ij}$. For the *M* ions in the present ODP's that can be either divalent or trivalent, the S_{ij} values were calculated for the both cases. For the Re ion, the bond-valence parameter d_0 that appeared in literature (1.86 Å)[16] was found not to give the reasonable V_i. Therefore, we have postulated the new parameter $d_0=1.91$ Å, so as to be consistent with the structural properties of Sr_2MgReO_6 and Sr_2ScReO_6, where the Re ions are obviously considered hexavalent and pentavalent, respectively.

Bond-valence data shown in Table I indicate that Re ions are hexavalent for $M=$ Mn, Co, Ni, Zn (as well as $M=$Mg by above definition) and pentavalent for $M=$Cr, and Fe (as well as $M=$Sc). Moreover, it is to be noted that Re ions for the metallic compounds (Sr_2CrReO_6, Sr_2FeReO_6, Ca_2FeReO_6) have relatively larger bond-valence sums than the insulating ones (Sr_2ScReO_6, Ca_2CrReO_6). This appears to reflect the mixed-valence nature of the metallic state.

Most of the Sr-based compounds have tetragonal symmetry except some monoclinic compounds ($M=$Sc, Mn, and Zn). In the latter compounds, relatively large ionic radii of these ions (Mn^{2+}: 0.83 Å, Sc^{3+}: 0.74 Å, and Zn^{2+}: 0.74 Å) may produce the monoclinic distortion. All the Ca-based compounds have monoclinic symmetry due to the small ionic radii of Ca^{2+}.

To see the trend of the tetragonal or monoclinic distortion, the cell volume, the monoclinic distortion as measured by $|\beta-90°|$ (β being the monoclinic angle), and the averaged *M*-O-Re bond angle in the ODP's are plotted against the tolerance factor t in Fig. 2. Here, the tolerance factor t is defined as $t=(r_a+r_o)/\sqrt{2}(r_b+r_o)$, where r_a, r_b, and r_o are average ionic radii for *A*, *B*, and O ions, respectively. To calculate t for Co^{2+} ion, an ionic radius for a Co^{2+} high-spin state was postulated.[8] Figure 2 also contains the data for Sr_2CaReO_6 ($M=$Ca) reported by Wiebe *et al.*[9] Apparently, the Sr-based compounds have larger cell volumes and larger *M*-O-Re angles (close to 180°) than the Ca-based compounds. For each *A*-site ion, the smaller-t compounds have larger cell volumes and smaller *M*-O-Re angles. The crystal lattice for $t<0.98$ compounds is monoclinically distorted and the distortion as measured by $|\beta-90°|$ increases with the decrease of t.

B. Electronic and magnetic properties

The electronic and magnetic properties are summarized in Table II for ODP's, A_2MReO_6 ($A=$Sr,Ca; $M=$Mg,Sc,Cr, Mn,Fe,Co,Ni,Zn). Ferromagnetic properties were observed for $M=$Cr, Mn, Fe, and Ni. Ca_2CoReO_6 also shows a ferromagnetic feature, yet the magnetization (*M*-*H*) curve does not saturate up to an applied magnetic field of 5 T. On the contrary, antiferromangetic features were observed for Sr_2ScReO_6 and Sr_2CoReO_6. Sr_2MgReO_6 and Sr_2ZnReO_6 also show antiferromagnetic properties, but their *M*-*H* curves exhibit a tiny hysteresis around zero field. It is worth

TABLE I. Lattice structural properties of ordered double perovskites A_2MReO_6 (A=Sr, Ca: M=Mg, Sc, Cr, Mn, Fe, Co, Ni, Zn) at room temperature. Here, a, b, and c ($a/\sqrt{2} \approx b/\sqrt{2} \approx c/2 = a_p$, a_p being the cubic perovskite lattice constant) are the lattice constants in tetragonal or monoclinic form in the unit of Å, and β is the monoclinic angle in the unit of degree. Cell volume and B-site order are in the unit of $Å^3$ and %, respectively. Re-Oi and M-Oi are the bond length between Re or M atom and ith oxygen in the unit of Å, and M-Oi-Re is the bend angle in the unit of degree. S_{ij} is bond-valence between the ith and jth atoms as defined as $S_{ij} = \exp\{(d_0 - d_{ij})/0.37\}$. Here, d_{ij} is the bond length between the ith and jth atoms and d_0 is the bond-valence parameter in unit of Å. V_i is the bond-valence sum calculated as $V_i = \Sigma_j S_{ij}$, indicating the effective valence of the ith metal element.

A	Sr	Sr	Sr	Sr	Sr	Sr	Sr	Sr	Sr	Ca	Ca	Ca	Ca
M	Mg	Sc	Cr	Mn	Fe	Co	Ni	Zn	Zn	Cr	Mn	Fe	Co
Rwp (%)	5.43	4.62	2.78	4.48	4.77	5.85	5.92	4.80	4.80	4.96	4.81	4.73	5.70
RI (%)	2.36	1.79	2.01	2.33	1.70	2.46	1.65	2.44	2.92	1.54	1.73	5.49	1.82
S(=Rwp/Re)	2.06	1.89	3.29	1.81	1.90	1.35	1.22	1.84	1.84	1.89	1.83	1.35	1.15
								85%	15%				
Symmetry	I4/m	P21/n	I4/m	P21/n	I4/m	I4/m	I4/m	I4/m	P21/n	P21/n	P21/n	P21/n	P21/n
a (Å)	5.56637(5)	5.67502(3)	5.52718(4)	5.66878(5)	5.56129(4)	5.56591(3)	5.54653(9)	5.57797(3)	5.63112(15)	5.38863(8)	5.44651(3)	5.40078(5)	5.40266(10)
b (Å)		5.65283(3)		5.64573(5)					5.59663(13)	5.46039(7)	5.63997(3)	5.52525(5)	5.57347(9)
c (Å)	7.93283(7)	7.98686(3)	7.80912(11)	7.99043(7)	7.9008(7)	7.95083(9)	7.91901(14)	8.00684(5)	7.90896(20)	7.65984(11)	7.77657(4)	7.6839(7)	7.68607(12)
β (deg)		90.0279(17)		89.9337(7)					90.065(3)	89.962(5)	90.1775(5)	90.0695(9)	89.7949(17)
Cell volume ($Å^3$)	245.8	256.2	238.6	255.7	244.4	246.3	243.6	249.1	249.3	225.4	238.9	229.3	231.4
B-site order (%)	100	100	76.7	100	100	100	100	100	100	86.3	100	100	100
M-O1 (Å)	2.0412(16)	2.037(4)	1.956(3)	2.1415(18)	1.985(7)	2.0529(16)	2.031(3)	2.0716(15)	2.061(11)	1.966(4)	2.1715(12)	2.025(2)	2.091(2)
M-O2 (Å)		2.038(4)		2.1370(19)					2.092(11)	1.973(4)	2.1416(14)	2.025(3)	2.096(2)
M-O3 (Å)	2.0468(19)	2.080(4)	1.956(6)	2.1328(24)	2.004(7)	2.062(2)	2.029(5)	2.085(18)	2.081(13)	1.956(6)	2.1343(13)	2.012(3)	2.064(3)
Re-O1 (Å)	1.9128(15)	1.990(4)	1.953(3)	1.9094(18)	1.961(7)	1.9112(16)	1.918(3)	1.9092(15)	1.932(11)	1.969(4)	1.9125(13)	1.959(3)	1.920(2)
Re-O2 (Å)		1.999(4)		1.9103(20)					1.905(11)	1.972(4)	1.9207(13)	1.954(2)	1.921(2)
Re-O3 (Å)	1.9196(19)	1.945(4)	1.949(6)	1.9098(24)	1.946(7)	1.914(2)	1.931(5)	1.9184(18)	1.906(13)	1.967(6)	1.9120(13)	1.940(3)	1.908(3)
M-O1-Re (deg)	169.08(5)	167.9(4)	179.7(18)	161.84(13)	170.22(5)	166.28(7)	166.69(6)	164.44(5)	167.6(11)	154.3(3)	147.38(7)	151.73(14)	150.72(14)
M-O2-Re (deg)		166.0(4)		162.48(13)					166.7(11)	153.1(3)	149.57(8)	152.24(14)	150.06(15)
M-O3-Re (deg)	180.0	165.48(9)	180.0	162.41(10)	180.0	180.0	180.0	180.0	165.4(4)	155.01(10)	147.82(7)	152.94(5)	150.68(11)
Bond-valence													
Re d_0 (Å)	1.91	1.91	1.91	1.91	1.91	1.91	1.91	1.91	1.91	1.91	1.91	1.91	1.91
S_{ij}	0.99	0.81	0.89	1.00	0.87	1.00	0.98	1.00	0.94	0.85	0.99	0.88	0.97
		0.79		1.00					1.01	0.85	0.97	0.89	0.97
	0.97	0.91	0.90	1.00	0.91	0.99	0.94	0.98	1.01	0.86	0.99	0.92	1.01
V_i	5.92	5.00	5.36	6.00	5.30	5.97	5.80	5.96	5.93	5.11	5.92	5.37	5.90
M^{3+} d_0 (Å)		1.849	1.708	1.732	1.713	1.637	1.750			1.708	1.732	1.713	1.637
S_{ij}		0.60	0.51	0.33	0.48	0.32	0.47			0.50	0.30	0.43	0.29
		0.60	0.51	0.33	0.48	0.32	0.47			0.49	0.33	0.43	0.29
		0.54	0.51	0.34	0.46	0.32	0.47			0.51	0.34	0.45	0.32
V_i		3.47	3.07	2.01	2.83	1.93	2.81			3.00	1.95	2.61	1.80
M^{2+} d_0 (Å)	1.693		1.730	1.765	1.751	1.685	1.670	1.704	1.704	1.730	1.765	1.765	1.685
S_{ij}	0.39		0.54	0.36	0.53	0.37	0.38	0.37	0.38	0.53	0.33	0.50	0.33
				0.37					0.35	0.52	0.36	0.50	0.33
	0.38		0.54	0.37	0.50	0.36	0.38	0.36	0.36	0.54	0.37	0.51	0.36
V_i	2.33		3.26	2.19	3.13	2.20	2.27	2.20	2.18	3.18	2.13	3.01	2.04

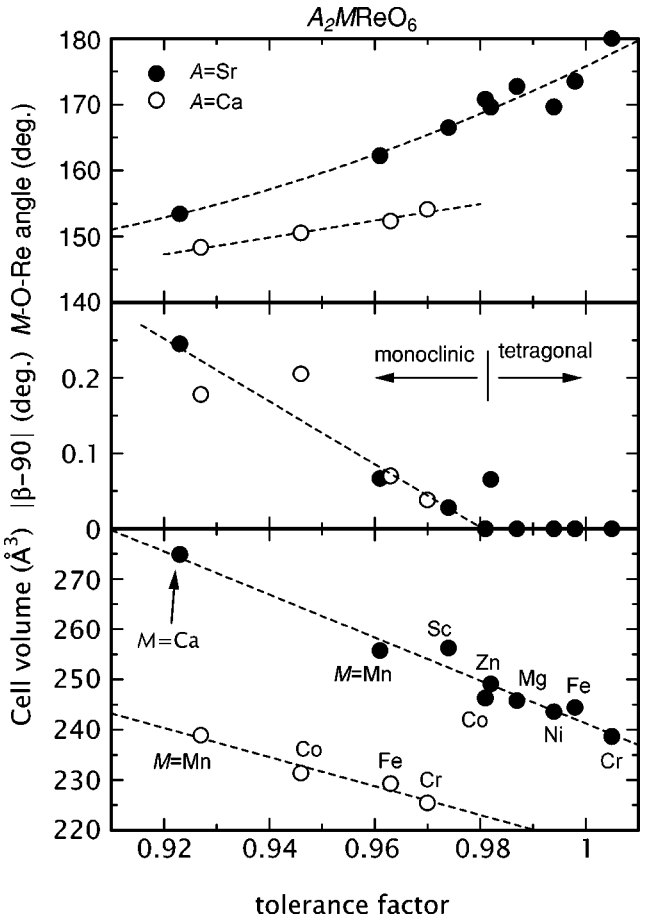

FIG. 2. Tolerance factor dependence of the cell volume, the monoclinic distortion as measured by $|\beta-90°|$ (β being the monoclinic angle), and the averaged M-O-Re bond angles for the ordered double perovskites A_2MReO_6 (A=Sr,Ca; M=Ca,Mg,Sc,Cr,Mn, Fe,Co,Ni,Zn). The figure contains the data for Sr_2CaReO_6 (M=Ca) cited from Ref. 9.

noting that the ferromagnetic impurities were scarcely observed in these compounds by the neutron diffraction measurements. It is reasonable to consider that they may arise from the spin canting of Re^{6+} ions or spin-glass-like ground state due to the geometrical frustration. The latter may be responsible for the small but finite electronic specific heat coefficient γ shown in Table II.

The resistivity (Fig. 3) and low-temperature specific-heat measurements (Fig. 4) confirmed a metallic nature of Sr_2FeReO_6 and Sr_2CrReO_6 (*vide infra*, see also Fig. 10). Figure 3 shows the temperature dependence of resistivity for ODP's, A_2MReO_6. For M=Mg, Sc, Mn, Ni, and Zn, i.e., for the Re^{6+}-based compounds, the resistivity at room temperature is in kΩcm-range irrespective of the A-site ions. The compounds with M=Co, Cr, and Fe or the nominally Re^{5+}-based compounds show relatively low resistivity. Among them, the A=Sr compounds have better conductivity than Ca-based ones. Temperature dependence of resistivity shows that all the compounds show an insulating nature except for Sr_2FeReO_6 and Sr_2CrReO_6. The latter two compounds have been assigned to the half-metals at the ground state.[2,11] Ca_2FeReO_6 undergoes a temperature-induced metal-insulator transition around 150 K accompanying an inflection point of resistivity curve (indicated by a triangle in Fig. 3), as reported previously.[10]

TABLE II. Magnetic, thermal, and electric properties of ordered double perovskites A_2MReO_6 (A=Sr,Ca; M=Mg,Sc,Cr,Mn,Fe, Co,Ni,Zn). F and AF represents ferromagnetism and antiferromagnetism, respectively. M_s, M_r, and H_c represent magnetization at an applied magnetic field of 5 T, spontaneous magnetization, and coercive force, respectively, and are measured at 4.2 K. T_C and T_N stand for ferromagnetic and antiferromagnetic transition temperature, respectively. γ indicate T-linear component of the low-temperature specific heat. M and I represents metal and insulator, respectively.

			Magnetic properties				Specific heat	Resistivity	
			M_s	M_r	H_c	T_c/T_N	γ		$\rho_{300\ K}$
A	M		μ_B	μ_B	T	K	mJ/K^{2}mol		Ωcm
Sr	Mg	AF		0.0005	0.2	320	0	I	1000
Sr	Sc	AF		0	0	75	3±1	I	1000
Sr	Cr	F	0.86	0.3	1.7	635	11±1	M	0.02
Sr	Mn	F	2.8	2.2	1.9	120	1±1	I	200
Sr	Fe	F	2.6	1.6	0.2	400	18±1	M	0.01
Sr	Co	AF		0	0	65	0	I	5
Sr	Ni	F	1	0.8	0.3	18	0	I	2000
Sr	Zn	AF		0.05	1.9	20	5±2	I	1000
Ca	Cr	F	0.8	0.43	3.1	360	3±1	I	0.34
Ca	Mn	F	0.9	0.5	4	110	0	I	100
Ca	Fe	F	2.2	1.6	0.8	525	4±1	M/I	0.03
Ca	Co	F	0.6	0.26	0.7	130	4±1	I	1000
Ca	Ni	F	0.2	0.1	2.8	140	0	I	1000

The low-temperature specific heat C for ODP's A_2MReO_6 (A=Sr,Ca; M=Mg,Sc,Cr,Mn,Fe,Co,Ni,Zn) is plotted as C/T versus T^2 in Fig. 4. Except for Sr_2NiReO_6, no clear magnetic transition was observed below 20 K in the T dependence of C of ODP's. Only for Sr_2NiReO_6, the broad peak corresponding to the ferromagnetic transition was observed around 18 K and it disappeared under a magnetic field of 5 T. The Schottky components C_s ($\propto 1/T^2$) caused by the Re nuclear moments are dominant below 1 K for some compounds; $(Sr,Ca)_2FeReO_6$, $(Sr,Ca)_2MnReO_6$ and

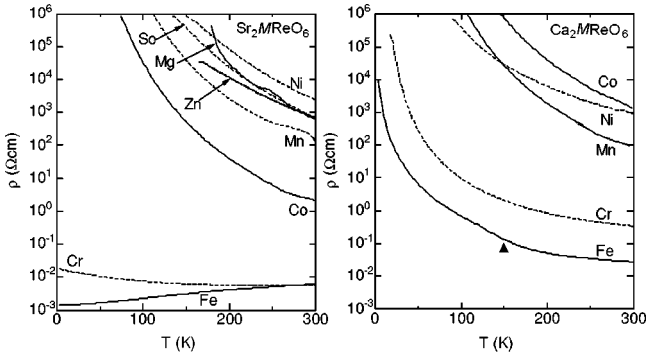

FIG. 3. Temperature (T) dependence of resistivity (ρ) for the ordered double perovskites A_2MReO_6 (A=Sr,Ca; M=Mg,Sc, Cr,Mn,Fe,Co,Ni,Zn).

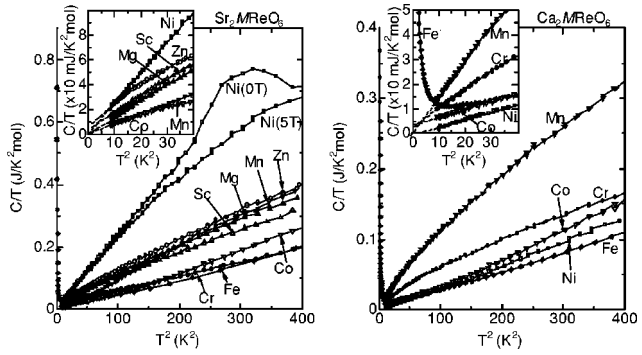

FIG. 4. The low-temperature specific heat C for ODP's, A_2MReO_6 (A=Sr,Ca; M=Mg,Sc,Cr,Mn,Fe,Co,Ni,Zn) plotted as C/T versus T^2. Insets show magnification of the low-temperature region. Dashed lines are merely the guides to the eyes.

Sr_2ScReO_6. The γ-values of $(Sr,Ca)_2FeReO_6$ were evaluated from the extrapolated $(C-C_s)/T$ values at 0 K.[10] For the other insulating and Sr_2CrReO_6 compounds, we confine the arguments to the data above 3 K (Ref. 17) and their γ values are estimated from the extrapolated C/T values at 0 K with and without a magnetic field 5 T,[18] as shown in the insets of Fig. 4 and Fig. 10. Table II summarizes the estimated γ values. The γ values reveal the metallic ground states for Sr_2MReO_6 (M=Fe,Cr) compounds and also the metal-insulator transitions with the change of A site to Ca. The small but finite γ values (3–5 mJ/K^{2}mol) for the insulating compounds of Sr_2MReO_6 (M=Sc,Zn) and Ca_2MReO_6 (M=Cr,Fe,Co) may be ascribed to glass state of spin or Re t_{2g} orbital and the associated subsisting enthalopy, as argued previously.[10,11]

The temperature dependencies of magnetization are shown in Fig. 5 for the ferromagnetic or ferrimagnetic ODP's, A_2MReO_6 (A=Sr,Ca; M=Cr, Mn, Fe, and Ni) under an applied magnetic field of 1 T. The saturation magnetizations for Sr_2MnReO_6 and Sr_2NiReO_6 were 2.8 and 1.0 μ_B/F.U., which are consistent with the values expected for the electronic configuration of Mn^{2+} (or Ni^{2+}) and Re^{6+}. For Ca_2MnReO_6 and Ca_2NiReO_6, the observed magnetizations at 1 T shown in Fig. 5 were quite low as compared with the value calculated by postulating the antiferromagnetic coupling between Mn^{2+} (or Ni^{2+}) and Re^{6+}. One of the reasons is the large coercive forces of these compounds (4.0 and 2.8 T, respectively). All these compounds show insulating nature and relatively low T_C ($<$150 K).

On the contrary, Sr_2CrReO_6 and Sr_2FeReO_6 with metallic nature have high magnetic T_C, 635 and 400 K, respectively. A large difference in T_C between the metallic and insulating compounds arises perhaps from presence or absence of the gap around the Fermi level, which should affect the effective exchange interaction between M and Re spins. The saturation magnetizations for Sr_2CrReO_6 and Sr_2FeReO_6 were 0.86 and 2.6 μ_B/F.U., respectively. These values are in accord with the electronic configuration of Cr^{3+} (or Fe^{3+}) and Re^{5+}, which should show 1 and 3 μ_B/F.U. in the simplest ionic model. The corresponding Ca-based compounds have the comparable saturation magnetization and high magnetic T_C, although Ca_2CrReO_6 shows an insulating nature, as

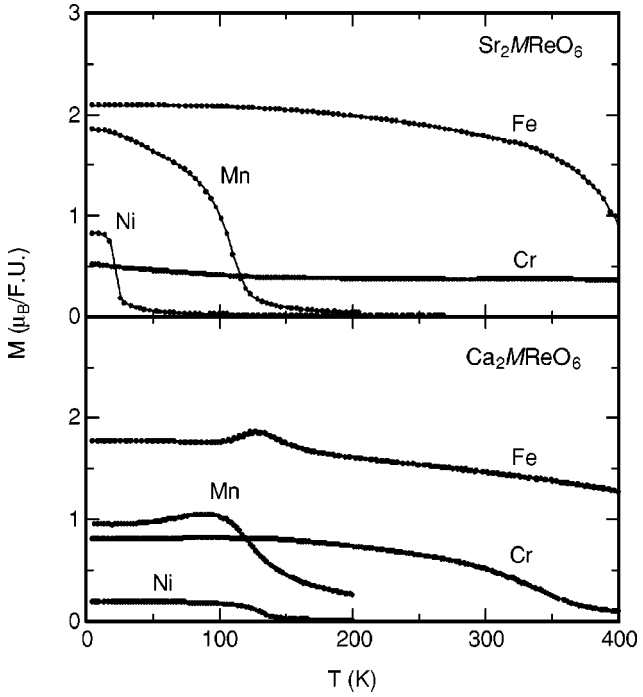

FIG. 5. Temperature (T) dependence of magnetization (M) at an applied magnetic field of 1 T for the ferromagnetic or ferrimagnetic A_2MReO_6 (A=Sr,Ca; M=Cr,Mn,Fe,Ni).

seen in Table II. The metal-insulator transition associated with the systematic change of T_C has been investigated by a previous study on the solid solution system, $(Sr,Ca)_2FeReO_6$.[10]

Figure 6 shows the inverse magnetization H/M for the antiferromagnetic ODP's A_2MReO_6 (A=Sr,Ca; M=Mg, Sc,Co,Zn). The results were obtained under a magnetic field of 1 T for M=Sc and Co, 0.1 T for M=Zn, and 0.01 T for M=Mg. Since Mg^{2+}, Sc^{3+}, and Zn^{2+} are nonmagnetic, only Re^{6+} (S=1/2) for M=Mg and Zn, or Re^{5+} (S=1) for M=Sc is relevant to the magnetism in these compounds. It is to be noted that the Re sites form the fcc lattice in ODP structure. Therefore, in the A_2MReO_6 with nonmagnetic M ion, the Re spins, S=1/2 for M=Mg and Zn and S=1 for M=Sc, may be subject to geometrical frustration. The frustration on the fcc lattice may cause rather complicated magnetic behaviors for these M=Mg, Sc, and Zn compounds as described below.

Sr_2ScReO_6 shows a Curie-Weiss-like behavior, although the susceptibility shows a temperature hysteresis around 30–80 K. The effective moment 1.08 μ_B/Re and Weiss temperature $\theta=-450$ K were obtained from the Curie-Weiss behavior. As compared with high Weiss temperature, the observed magnetic transition (T_N=75 K) is considerably low, indicating the long-range magnetic order may be suppressed by the aforementioned geometrical frustration. The hysteretic behavior around T_N suggests the first-order nature in the transition. This may arise from the concomitant occurrence of the lattice structural transition that may lift the degeneracy. The detailed structural variation around T_N deserves to be studied.

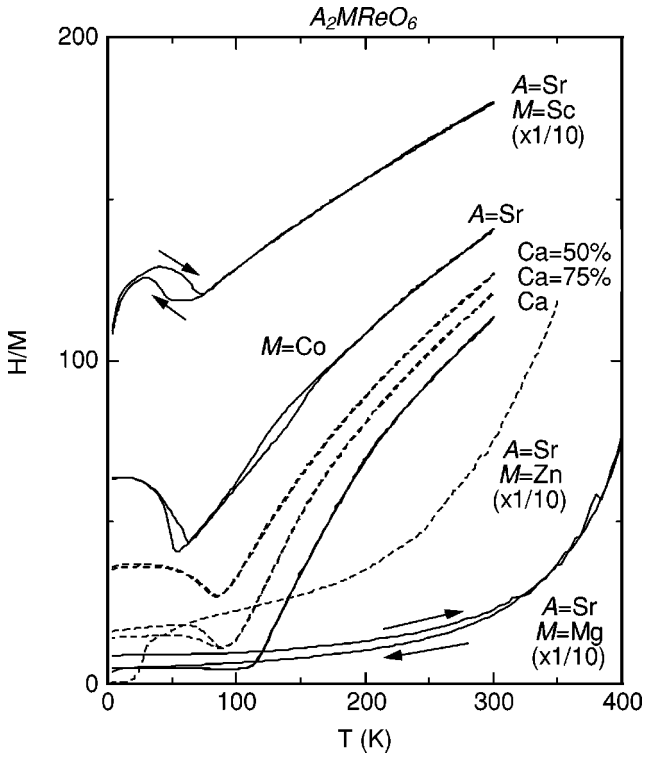

FIG. 6. Temperature (T) dependence of inverse magnetization (H/M) for the antiferromagnetic A_2MReO_6 (A=Sr,Ca; M=Mg, Sc,Co,Zn). The applied magnetic field is $\mu_0H=1$ T except for M=Mg ($\mu_0H=0.01$ T) and Zn ($\mu_0H=0.1$ T).

On the other hand, Sr_2MgReO_6 and Sr_2ZnReO_6 with $S=1/2$ spins on the fcc lattice have a small but finite spontaneous magnetization, and the temperature dependence of H/M curve shows a thermal hysteresis below 320 K for Sr_2MgReO_6. Its structure and magnetic properties were reported also by Wiebe *et al.*[19] Below 20 K, Sr_2ZnReO_6 shows an increased spontaneous magnetization and a large coercive force ($0.05\mu_B$ and 1.9 T at 4.2 K, respectively), indicating that the long-range magnetic ordering sets in around this temperature. The origin of such a week ferromagnetism is left to be elucidated.

The magnetization curves for $(Sr_{1-y}Ca_y)_2CoReO_6$ (y=0.0,0.5,0.75,1.0) are shown in Fig. 7. $(Sr_{1-y}Ca_y)_2CoReO_6$ shows an antiferromagnetic feature for $y=0.0$ and 0.5, while ferromagnetic for $y=1.0$. At $y=0.75$, the compound shows a complicated behavior. Nevertheless, the magnetization increases almost linearly with increasing the magnetic field for all the compounds. The H/M vs T curves for these compounds tend to show a change in slope with increasing temperature as shown in Fig. 6. These features resemble those observed for Ba_2CoReO_6 with helical spin order, in which Co and Re sublattice moments in a given (001) plane are coupled antiparallel, and successive planes undergo a rotation about 100°.[8] This implies the occurrence of a similar helical spin order also in $(Sr_{1-y}Ca_y)_2CoReO_6$. Since we observed no magnetic impurities but magnetic reflection at $d=7.68$ Å for $y=1$ (Ca_2CoReO_6) compound by the powder neutron diffraction measurements,[20] the ferromagnetic component observed for

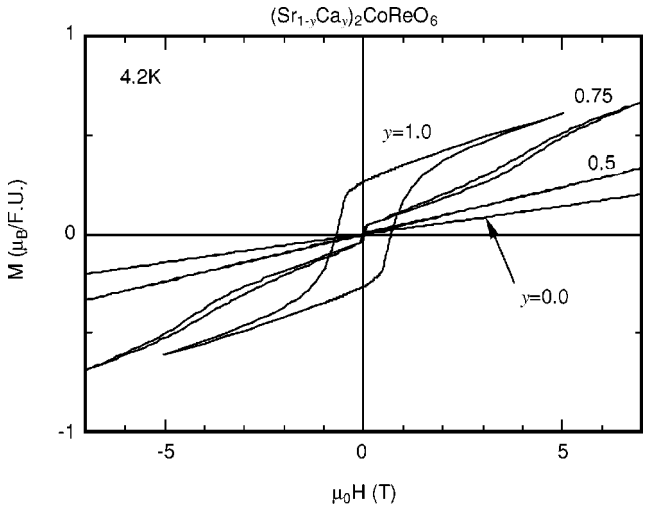

FIG. 7. Magnetization curves for $(Sr_{1-y}Ca_y)_2CoReO_6$ ($y=0.0$, 0.5, 0.75, and 1.0) at 4.2 K.

$y>0.75$ is likely due to the conical spin structure that is perhaps affected by the monoclinic distortion induced by increment of Ca content.

C. Metal-insulator phenomena

A schematic diagram of the electron configurations of B-site ions is shown in Fig. 8 for ferrimagnetic ODP's A_2MReO_6 (M=Cr,Mn,Fe,Ni). On the basis of this scheme, qualitative explanation may be given for metal-insulator phenomena of ODP's as follows: For Fe^{3+} ($3d^5$) and Cr^{3+} ($3d^3$), the added electron will reside on the t_{2g} down-spin state, which is also the case for Re^{6+} ($5d^1$). Therefore, the both t_{2g} bands of M=(Cr,Fe) and Re can hybridize with each other, allowing the hopping of down-spin electron between the Re^{5+} and Fe^{3+} (Cr^{3+}) sites or between the Re^{6+} and Fe^{2+} (Cr^{2+}) sites. In other words, the down-spin t_{2g} hybridized band locates around the Fermi en-

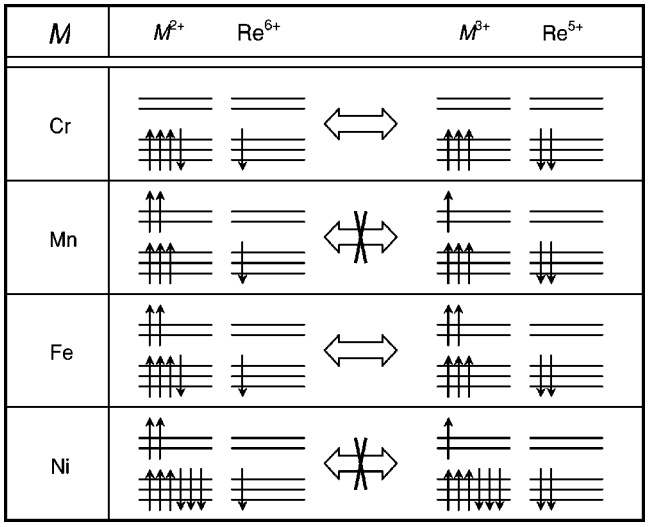

FIG. 8. Possible electron configurations of B-site ions for ferrimagnetic A_2MReO_6 (M=Cr,Mn,Fe,Ni). Thick arrows with and without cross means the forbidden and allowed valence fluctuation, respectively (see the text).

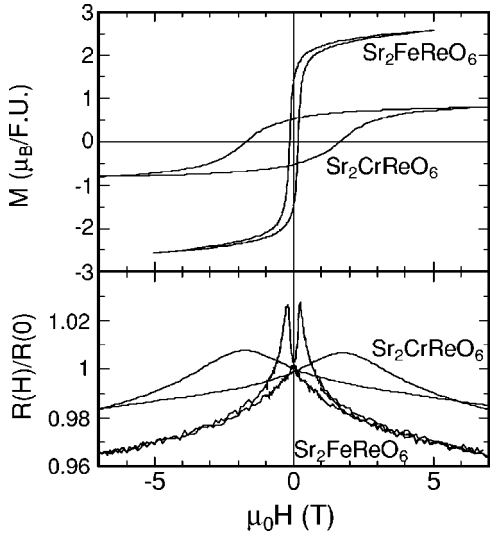

FIG. 9. Magnetization (M) and magnetoresistance $R(H)/R(0)$ against applied magnetic field H at 4.2 K for metallic ordered double perovskites Sr_2MReO_6 (M=Cr,Fe). Resistance $R(H)$ was normalized by the zero-field value $R(0)$.

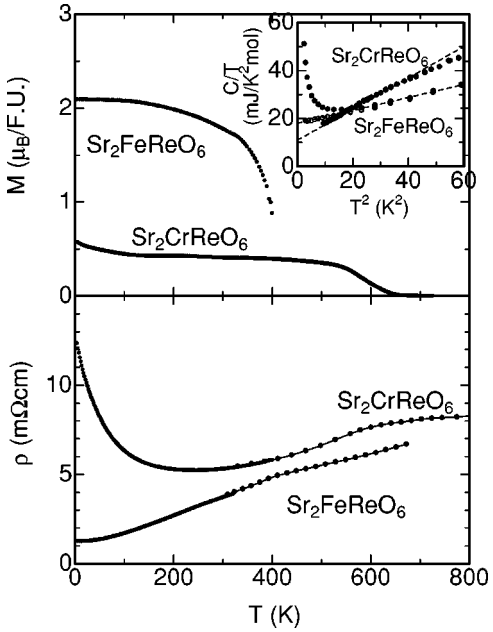

FIG. 10. Temperature (T) dependence of magnetization (M) at 1 T and resistivity (ρ) for metallic ordered double perovskites: Sr_2MReO_6 (M=Cr,Fe). Inset shows the low-temperature specific heat C plotted as C/T versus T^2. The open circles shows $(C-C_s)/T$ versus T^2 for Sr_2FeReO_6, where the Schottky term C_s caused by Re nuclear moments is subtracted.

ergy because of such a mixed-valence character, thus forming a half-metallic conduction band. This intuitive explanation is confirmed by the first-principles electronic calculation for Sr_2FeReO_6.[2] In Ca_2FeReO_6 and Ca_2CrReO_6, however, the lattice distortion makes the one-electron bandwidth smaller than in their Sr analogs, placing the compounds close to the Mott transition, i.e., the electron-correlation induced metal-insulator transition. In previous studies,[10,11] we have reported that Ca_2CrReO_6 shows an insulating nature and that Ca_2FeReO_6 undergoes the metal-insulator transition at around 150 K.

On the contrary to the above case, the highest occupied state for Mn^{2+} and Ni^{2+} is the up-spin e_g state. To virtually excite the M^{3+}-Re^{5+} state, the up-spin e_g electron on M^{2+} has to move to the down-spin t_{2g} state on Re^{6+}. Because of zero mixing between t_{2g} and e_g states on the neighboring sites in ideal cubic perovskite, such a transfer process is almost forbidden in the ODP structure. Note that the electron configuration of Mn^{2+}-Re^{6+} is nearly identical with that of the half-metallic Fe^{3+}-Mo^{5+} combination.[1] Nevertheless, Mn^{2+}-Re^{6+} shows an insulating nature perhaps because the energy of the Mn^{1+}-Re^{7+} state is too high to produce the effective mixed-valence state. This small hybridization makes this compound insulating (Mott insulator).

Figure 9 shows the magnetization and magnetoresistance (MR) plotted against the applied magnetic field for metallic ODP's Sr_2MReO_6 (M=Cr, Fe) at 4.2 K in polycrystalline form. MR was normalized by the resistance at 0 T, such as $R(H)/R(0)$. The negative MR was observed, about 6% and 3% for Sr_2FeReO_6 and Sr_2CrReO_6, respectively. The resistance peaks were observed at 0.2 and 1.8 T for Sr_2FeReO_6 and Sr_2CrReO_6, respectively, which will correspond to the M=0 points (coercive forces) of the respective magnetization curves. These results indicate that the observed MR is caused by the spin scattering at the grain boundaries of the polycrystalline compounds, i.e., the intergrain tunneling MR.

The temperature (T) dependence of magnetization (M) and resistivity (ρ) is shown in Fig. 10 for metallic Sr_2FeReO_6 and Sr_2CrReO_6. The inset shows the low-temperature specific-heat (C) plotted as C/T versus T^2. The onset of the ferromagnetic magnetization is observed around T_C=400 and 635 K for Sr_2FeReO_6 and Sr_2CrReO_6, respectively. With decreasing temperature below T_C, the magnetization arises and the resistivity tends to decrease perhaps due to the reduction of carrier scattering by thermally agitated spins. The electronic specific-heat coefficient γ estimated from low temperature specific heat was about 18 and 11 mJ/K^{2}mol for Sr_2FeReO_6 and Sr_2CrReO_6, respectively, which also indicates a metallic nature of the both compounds.

IV. CONCLUSION

Lattice structures of a series of Re-containing ODP's, A_2MReO_6 (A=Sr,Ca; M=Mg,Sc,Cr,Mn,Fe,Co,Ni,Zn), have been investigated by powder neutron diffraction measurements. In terms of the bond-valence sum calculated from the deduced Re-O bond lengths, the Re ion in the ODP is assigned as essentially pentavalent (5+) for M=Sc, Cr, and Fe and hexavalent (6+) for M=Mg, Mn, Co, Ni, and Zn. However, the Re valence for the M=Cr and Fe compounds as measured by the bond-valence sum method is +5.3–+5.4, indicating a mixed-valence (both Re^{5+}/Re^{6+} and Cr^{3+}/Cr^{2+} or Fe^{3+}/Fe^{2+}) character. All these M=Cr and Fe compounds are close to the metal-insulator boundary. In particular, Sr_2CrReO_6 and Sr_2FeReO_6 are ferromagnetic metals, perhaps half-metals at the ground state, with high magnetic

transition temperatures of 635 and 400 K, respectively. The low-temperature specific-heat data as well as the transport ones have revealed the metallic ground states for these Sr_2MReO_6 (M=Fe,Cr) compounds and also the metal-insulator transition with the change of A site to Ca. The intergrain tunneling type magnetoresistance has been confirmed for the prospective half-metallic compounds, Sr_2CrReO_6 and Sr_2FeReO_6.

ACKNOWLEDGMENTS

The present work was in part supported by a Grant-In-Aid for Scientific Research from the MEXT, Japan. One of the authors (T.O.) is grateful for the support from the Iwatani Naoji Foundation's Research Grant and the Mazda Foundation's Research Grant.

*Present address: Fuji Electric Advanced Technology Co. Ltd., Hino-city 191-8502, Japan.

†Present address: Department of Nano-structures and Advanced Materials, Kagosima University, Kagoshima 890-0065, Japan.

‡Present address: Center for Proton Accelerator Facility, Japan Atomic Energy Research Institute (JAERI), Tokai-mura, Ibaraki-ken 319-1195, Japan.

[1] K.-I. Kobayashi, T. Kimura, H. Sawada, K. Terakura, and Y. Tokura, Nature (London) **395**, 677 (1998).

[2] K.-I. Kobayashi, T. Kimura, Y. Tomioka, H. Sawada, K. Terakura, and Y. Tokura, Phys. Rev. B **59**, 11 159 (1999).

[3] T.H. Kim, M. Uehara, S-W. Cheong, and S. Lee, Appl. Phys. Lett. **74**, 1737 (1999).

[4] G. Blasse, *Proceedings of the International Conference on Magnetism, Nottingham 1964* (Institute of Physics and the Physical Society, London, 1965), p. 350.

[5] M. Itoh, I. Ohta, and Y. Inaguma, Mater. Sci. Eng., B **41**, 55 (1996).

[6] A.W. Sleight, J. Longo, and R. Ward, Inorg. Chem. **1**, 245 (1962).

[7] A.W. Sleight, and J.F. Weiher, J. Phys. Chem. Solids **33**, 679 (1972).

[8] C.P. Khattak, D.E. Cox, and F.F.Y. Wang, AIP Conf. Proc. **10**, 674 (1973).

[9] C.R. Wiebe, J.E. Greedan, G.M. Luke, and J.S. Gardner, Phys. Rev. B **65**, 144413 (2002).

[10] H. Kato, T. Okuda, Y. Okimoto, Y. Tomioka, K. Oikawa, T. Kamiyama, and Y. Tokura, Phys. Rev. B **65**, 144404 (2002).

[11] H. Kato, T. Okuda, Y. Okimoto, Y. Tomioka, Y. Takenoya, A. Ohkubo, M. Kawasaki, and Y. Tokura, Appl. Phys. Lett. **81**, 328 (2002).

[12] T. Kamiyama, S. Torii, K. Mori, K. Oikawa, S. Itoh, M. Furusaka, S. Satoh, T. Egami, S. Ikeda, F. Izumi, and H. Asano, Mater. Sci. Forum **321-324**, 302 (2000).

[13] T. Kamiyama, K. Oikawa, N. Tsuchiya, M. Osawa, H. Asano, N. Watanabe, M. Furusaka, S. Satoh, I. Fujikawa, T. Ishigaki, and F. Izumi, Physica B **213-214**, 875 (1995).

[14] T. Ohta, F. Izumi, K. Oikawa, and T. Kamiyama, Physica B **234-236**, 1093 (1997).

[15] N.E. Brese and M. O'keeffe, Acta Crystallogr., Sect. B: Struct. Sci. **47**, 192 (1991).

[16] I.D. Brown, bvparm.cif, available at http://ccp14.minerals.csiro.au/ccp/web-mirrors/i_d_brown/bond_valence_param/

[17] For the insulating compounds and Sr_2CrReO_6, the low-temperature specific heat data below 3 K, measured by a relaxation method, were not reliable, because a double thermal relaxation were observed due to the thermal resistances between sample and substrate of a cell. In this paper, except for $(Sr,Ca)_2FeReO_6$, we confine the arguments to the data above 3 K, in which the contribution of nuclear Schottky components is negligible.

[18] Y. Tomioka, T. Okuda, Y. Okimoto, R. Kumai, K.-I. Kobayashi, and Y. Tokura, Phys. Rev. B **61**, 422 (2000).

[19] C.R. Wiebe, J.E. Greedan, P.P. Kyriakou, G.M. Luke, J.S. Gardner, A. Fukaya, I.M. Gat-Malureanu, P.L. Russo, A.T. Savici, and Y.J. Uemura, Phys. Rev. B **68**, 134410 (2003).

[20] K. Oikawa, T. Kamiyama, H. Kato, and Y. Tokura (unpublished).